(11) Sugie, T.; Hiltner, A. *J. Macromol. Sci., Phys.* **1980**, *B17*, 769–785.
(12) Hayashi, T.; Walton, A. G.; Anderson, J. M. *Macromolecules* **1977**, *10*, 346–351.
(13) Doty, P.; Bradbury, J. H.; Holtzer, A. M. *J. Am. Chem. Soc.* **1956**, *78*, 947–954.
(14) Flory, P. J. "Principles of Polymer Chemistry"; Cornell University Press: Ithaca, N.Y., 1953; p 580.
(15) Hayashi, T.; Anderson, J. M.; Hiltner, P. A. *Macromolecules* **1977**, *10*, 352–356.
(16) Fasman, G. D.; Hoving, H.; Timasheff, S. N. *Biochemistry* **1970**, *9*, 3316–3324.

Hydrogen-Bonding Properties of Hard-Segment Model Compounds in Polyurethane Block Copolymers

C. M. Brunette, S. L. Hsu,* and W. J. MacKnight

Polymer Science and Engineering Department, Materials Research Laboratory, University of Massachusetts, Amherst, Massachusetts 01003. *Received June 5, 1981*

ABSTRACT: The N–H stretching vibration in three model hard-segment compounds for polyurethane block copolymers based on 2,4- and 2,6-toluene diisocyanate (TDI) and *p,p'*-diphenylmethane diisocyanate (MDI) with 1,4-butanediol has been studied by infrared spectroscopy. Changes in the frequency, half-width, and integrated intensity resulting from thermal treatment have been correlated to the degree of structural organization as evidenced by differential scanning calorimetry (DSC). The temperature dependence of hydrogen bonding in these materials was also investigated.

Introduction

Segmented polyurethanes are a class of materials consisting of alternating hard- and soft-segment units. The hard segments are commonly based on *p,p'*-diphenylmethane diisocyanate (MDI), 2,6- or 2,4-toluene diisocyanate (TDI), and butanediol (BD) whereas the soft segments are typically low molecular weight polyesters or polyethers. Segregation of the hard-segment units into domains is believed to be responsible for their unusual properties (i.e., enhanced modulus, high extensibility, and resiliency) and morphologies.[1-3]

Such polyurethanes are extensively hydrogen bonded. In all cases, the N–H group of the urethane serves as the proton donor while the acceptor group may include the carbonyl and adjacent oxygen atom in the urethane group as well as the ester carbonyl or ether oxygen of the soft segment. Although hydrogen bonding is an important structural feature of segmented polyurethanes, its influence on their properties and morphologies is not clear. Working on a series of MDI-based polyurethanes, Cooper et al.[4] have concluded that the thermal behavior of hydrogen bonding is independent of morphology and depends primarily on the glass transition temperature of the hard segments. Investigations by the X-ray diffraction method[5,6] of hydrogen bonding and the orientation mechanisms of segmented polyurethanes have suggested otherwise; both crystallization of the hard segments and the observed orientation behavior have been explained by "restructuring" of the physical cross-linking caused by hydrogen bonding.

While hydrogen bonding in segmented polyurethanes has been the subject of numerous investigations using infrared spectroscopy, very little systematic interpretation has so far been made of the spectral features associated with the N–H absorption band. As in most hydrogen-bonded systems, this stretching mode displays well-known and characteristic perturbations: frequency shift, increase in bandwidth relative to the natural width, and enhancement of intensity. The frequency shift has been generally accepted as a measure of the strength of the hydrogen bond, correlating well to hydrogen bond energy[7] and

Chart I

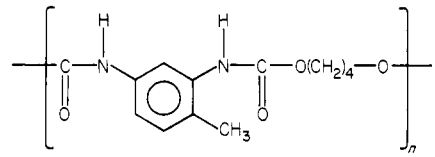

2,4-TDI-BD

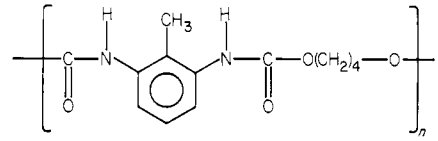

2,6-TDI-BD

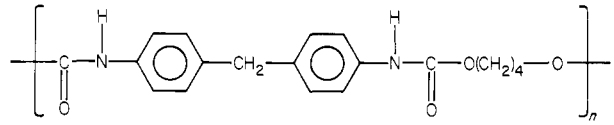

MDI-BD

NH---O distance in solids.[7-10] Although the origin of the latter two effects is less clear, changes in these properties are no doubt indicative of the structural and hydrogen-bonding features of these systems and may therefore lead to additional information about the effects of hydrogen bonding on morphology.

The present work is concerned with a detailed analysis of the N–H stretching vibration in three copolymers based on MDI, 2,6-TDI, and 2,4-TDI polymerized with butanediol (BD). They were selected to be representative of the chemical structures and morphologies of the hard-segment units in polyurethane elastomers. As in those materials, the 2,4-TDI–BD copolymer is completely amorphous[11] while 2,6-TDI–BD and MDI–BD are capable of crystallizing under the proper conditions.[11,12] It was therefore of interest to examine changes in the spectroscopic properties of the N–H vibration after annealing and determine whether additional information on the nature of hydrogen bonding and chain packing could be obtained from this type of analysis. The temperature dependence of hydrogen

0024-9297/82/2215-0071$01.25/0

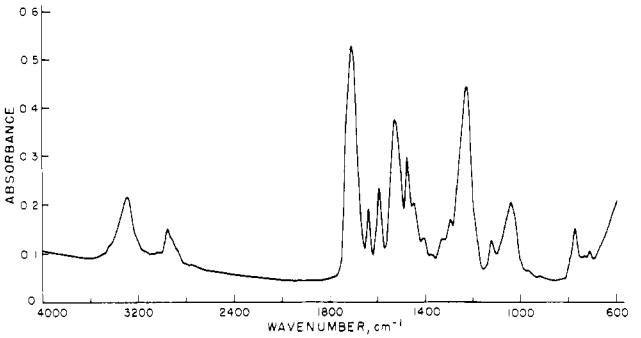

Figure 1. Survey infrared spectrum of model hard-segment compound 2,4-TDI–BD.

bonding in these materials is also investigated. The results will be interpreted in light of current views on hydrogen-bonded systems and compared to differential scanning calorimetry (DSC) studies.

Materials and Methods

The three model compounds were synthesized from 1,4-butanediol (BD) and each of the following diisocyanates: 2,4-toluene diisocyanate (2,4-TDI), 2,6-toluene diisocyanate (2,6-TDI), and *p,p'*-diphenylmethane diisocyanate (MDI) (Chart I). The solution polymerization of these polymers was carried out in a 50:50 mixture of dimethyl sulfoxide and methyl isobutyl ketone following a procedure described by Lyman.[13]

Infrared spectra (400–4000 cm^{-1}) were obtained with a Nicolet 7199 Fourier transform infrared spectrometer. Two hundred scans at 2-cm^{-1} resolution were signal averaged and stored on a disk for further analysis. Samples were prepared by solution casting 5% (w/v) polymer from *N,N*-dimethylformamide (DMF) directly onto KBr plates and vacuum drying for 4 days at 50 °C. Survey spectra did not show any evidence of residual solvent (see Figure 1). The three samples were then placed in a vacuum oven and annealed at 150 °C. Spectra were collected after various annealing times ranging from 30 min to 8 h.

Since rapid solvent evaporation is thought to be responsible for the lower melting points and heats of fusion of the solution-cast MDI–BD copolymer compared to the as-polymerized material,[14] a second drying procedure was used to circumvent this problem and facilitate crystallization. Here the KBr plate containing the polymer solution (5% w/v) was mounted in an evaporating dish, the bottom of which was covered with filter paper and saturated with DMF. The dish was then covered and placed in an oven for 24 h at 100 °C. Again no residual solvent was detected in the infrared spectrum.

For the temperature scans, the sample was placed in a variable-temperature unit (Wilks Model no. 19) connected to the temperature controller (Wilks Model no. 37) and the temperature was monitored by a copper–constantan thermocouple junction placed directly on the sample. The temperature was held constant for about 5 min before spectra were collected. A dry nitrogen flow was maintained over the film throughout the measurements to avoid the condensation of moisture on the salt plate.

In the infrared analyses, absorption frequencies are accurate to ±1 cm^{-1} and widths at half peak height to about ±5 cm^{-1}. Frequency shifts are listed as $\Delta\nu = \nu_f - \nu_b$, where ν_f and ν_b are the frequencies of maximum absorption for the free and bonded N–H groups, respectively. Integrated intensities have been corrected for sample thickness differences using the CH_2 stretch near 2950 cm^{-1} as normalizing factors. These vibrational modes are very localized and, therefore, suitable for quantitative analysis.[15] The fraction of hydrogen-bonded N–H groups, X_b, is determined by a curve-resolving technique based on a nonlinear least-squares analysis for the fitting of a combination of Lorentzian and Gaussian curve shapes. Values are reliable to within ±1%. The extinction coefficient difference between the free and bonded N–H absorption is also taken into account in the analyses.[16,17]

Differential scanning calorimeter data were obtained on a Perkin-Elmer DSC-2. Runs were conducted on polymer samples of about 15 mg at a heating rate of 20 °C/min. The cell was calibrated for quantitative measurements using indium and tin standards. As in the infrared studies, polymers were cast from DMF solution (5% w/v) and subjected to the same thermal treatment.

Table I
Band Assignments for Hard-Segment Model Compounds

frequency, cm^{-1}	assignment[a]
	ν(N—H), free N–H
3450	in 2,6- and 2,4-TDI
3420	in MDI
	ν(N—H), bonded N—H
3330	in MDI
3310	in 2,4-TDI
3300	in 2,6-TDI
1735	ν(C=O), free C=O
	ν(C=O), bonded C=O
1708	in 2,4-TDI
1706	in 2,6-TDI
1703	in MDI
	δ(N—H) + ν(C—N)
1530	in MDI
1523	in 2,6- and 2,4-TDI
	δ(N—H) + ν(C—N)
1240	in 2,6-TDI
1230	in MDI
1225	in 2,4-TDI
1080	ν(C—O—C) in $-\overset{O}{\overset{\|}{C}}-O-C$
774	$\gamma(-\overset{O}{\overset{\|}{C}}-O-)$

[a] ν = stretching, δ = in-plane bending, and γ = out-of-plane bending.

Table II
Changes of N—H Stretching Vibration as a Function of Annealing Time

annealing time	$\Delta\nu$, cm^{-1}	$\nu_{1/2}$, cm^{-1}	I^a
	2,6-TDI-BD		
0	150	105	3.75
30 min	152	102	3.95
90	169	92	4.35
4 h	170	66	4.67
8 h	172	58	4.82
	2,4-TDI-BD		
0	140	107	3.50
90 min	140	109	3.42
4 h	140	111	3.30
8 h	140	111	3.20
	MDI-BD		
0	90	92	3.09
90 min	90	92	3.21
4 h	88	88	3.23
8 h	88	88	3.26
24 h[b]	102	56	4.10

[a] Normalized with respect to the 2950-cm^{-1} CH stretching vibration. [b] Slow solvent evaporation technique.

Results

Infrared. All polymers when cast from DMF solution produced transparent films. Figure 1 shows a typical infrared spectrum (4000–600 cm^{-1}) of these materials. Although several vibrations are involved in hydrogen bonding, i.e., carbonyl stretching (amide I), N–H in-plane bending (amide II), and out-of-plane deformation (amide V) (see Table I), this study is principally concerned with the N–H stretching vibration. In each spectrum, the strong

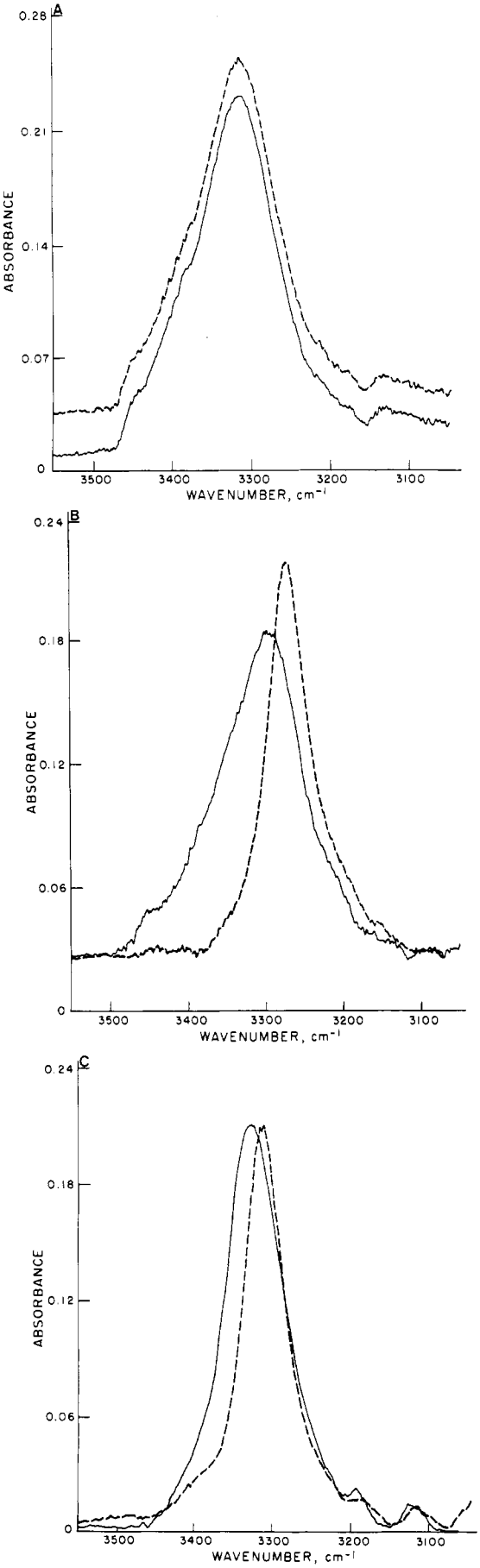

Figure 2. Effect of annealing on the N–H absorption of model hard-segment compounds: (A) 2,4-TDI–BD; (B) 2,6-TDI–BD; (C) MDI–BD; (——) control; (– – –) annealed at 150 °C for 8 h in (A) and (B) and slow solvent evaporation technique in (C).

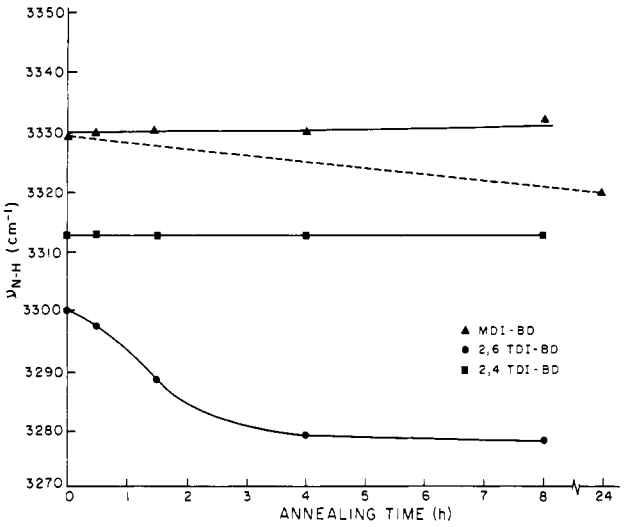

Figure 3. Effect of annealing time on the position of the N–H absorption (ν_{NH}) in model hard-segment compounds; (– – –) slow solvent evaporation technique.

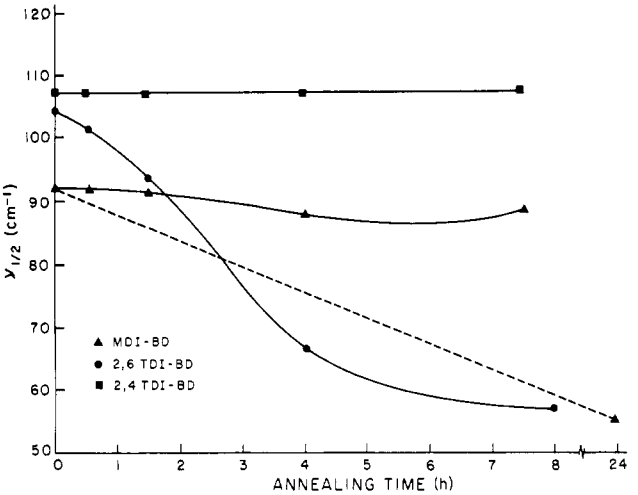

Figure 4. Effect of annealing time on the half-width ($\nu_{1/2}$) of the N–H absorption in model hard-segment compounds; (– – –) slow solvent technique.

absorption peak centered around 3300 cm^{-1} is assigned to the hydrogen-bonded N–H groups while the weak shoulder on the high-frequency side of this peak corresponds to the free N–H groups. The spectral properties relating to this vibration are summarized in Table II.

Prior to annealing, it is clear that the half-widths, $\nu_{1/2}$, frequency shift, $\Delta\nu$, and integrated intensities, B, of the N–H stretch are of comparable magnitude in the 2,4- and 2,6-TDI–BD copolymers; $\nu_{1/2}$ is in the range 100–110 cm^{-1}, $\Delta\nu$ about 150 cm^{-1}, and B, 3.6. The smaller values obtained in MDI–BD are presumably due to steric factors associated with packing. In agreement with earlier studies on the corresponding polyurethanes and model systems,[16-18] 80–85% of the N–H groups are found to be hydrogen bonded in these materials.

Qualitative changes in the N–H absorption region after annealing are shown in Figure 2. Annealing at 150 °C for as long as 8 h produced no change in the intensity, shape, or position in the 2,4-TDI–BD copolymer. In contrast, the N–H stretching vibration in 2,6-TDI–BD exhibited nearly a 50% reduction in half-width for the annealed sample. When compared to the initial solution-cast material, there is also a 22-cm^{-1} shift in position to lower frequencies as well as an increase in intensity. These spectral properties are plotted as a function of annealing time in Figures 3–5.

Table III
DSC Events as a Function of Annealing Time

annealing time	peak, °C							
	2,6-TDI-BD			MDI-BD				2,4-TDI-BD
control	92[a]	160	195	94	135	200	217	101
90 min		160	207			202	227	104
4 h		187	214			210		102
8 h		195	218			210		102
24 h[b]						225	231	

[a] Uncertainty for each temperature is ±2 °C. [b] Slow solvent evaporation technique.

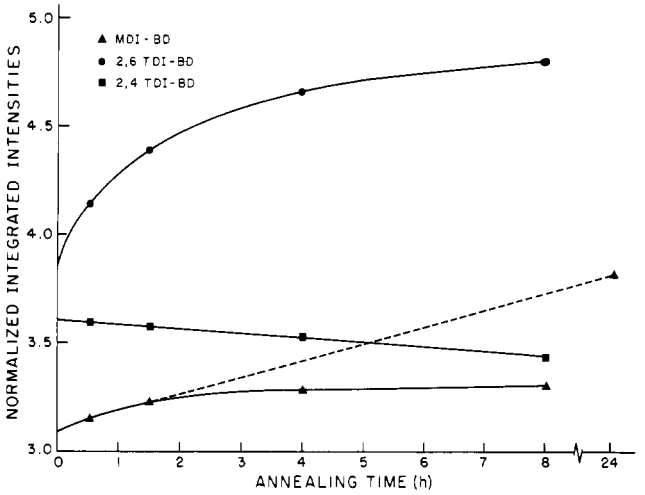

Figure 5. Effect of annealing time on the normalized integrated intensity (B) of the N–H absorption in model hard-segment compounds; (---) slow solvent evaporation technique.

It is noted that the most significant changes occur during the first 3 h of annealing in the 2,6-TDI copolymer after which these properties approach a nearly constant value. Similar changes are also observed in the carbonyl region of the 2,6-TDI–BD spectrum; the bonded C=O component decreases by 12 cm^{-1} and narrows. Consistent with this decrease in the stretching frequency, the bending vibrations at 1530 and 760 cm^{-1} increase 2–3 cm^{-1}. The band shapes, however, remain essentially unchanged.

The magnitudes of the spectral changes observed for MDI–BD are very sensitive to the annealing conditions. While a slight narrowing (<10 cm^{-1}) and frequency shift (2–3 cm^{-1}) are observed in samples annealed at 150 °C, more dramatic changes occur in the slowly evaporated cast sample. Here the half-width of the N–H stretching vibration decreases by 36 cm^{-1} and the frequency by 12 cm^{-1}. The intensity also increases, comparable to the increase observed in the 2,6-TDI–BD sample. It is noted that these spectral changes are not accompanied by any measurable change in the fraction of hydrogen-bonded N–H groups.

DSC. All hard-segment copolymers display a glass transition, T_g, between 90 and 100 °C. These values are in good agreement with those reported in the literature.[19,20] In addition, very weak transitions are observed for the 2,6-TDI–BD and MDI–BD samples between 135 and 200 °C.

Figure 6 shows the DSC scans for 2,6-TDI–BD following heat treatment. After 90 min of annealing, the lower transition T_g is no longer discernible but a broad and well-defined endotherm appears at 207 °C in addition to the weak endotherm at 160 °C. At longer annealing times, both endotherms progressively shift to higher temperatures and become sharper. After a total of 8 h of annealing, the lower transition occurs at 195 °C while the main peak has shifted to 218 °C. Similar to the intensity variation of the N–H stretching vibration, the area under the melting peak

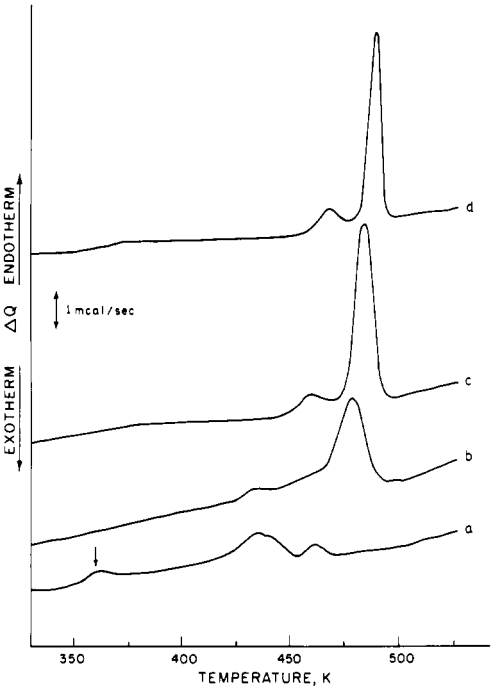

Figure 6. DSC curves for 2,6-TDI–BD annealed at 150 °C: (a) control; (b) 90 min; (c) 4 h; (d) 8 h.

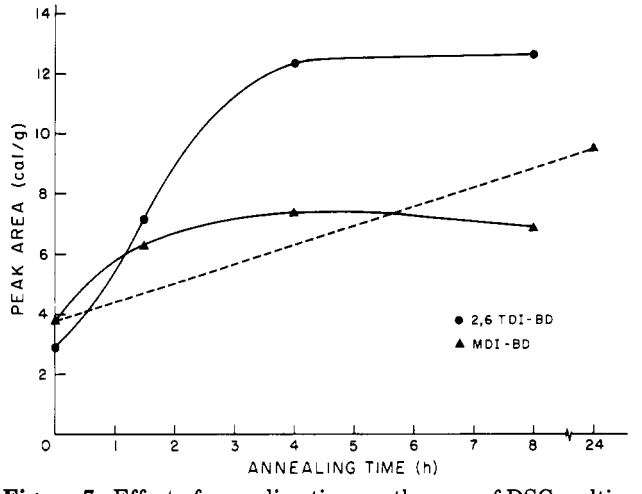

Figure 7. Effect of annealing time on the area of DSC melting peaks; (---) slow solvent evaporation technique.

increases rapidly during the first 3 h of annealing after which it approaches a nearly constant value (see Figure 7). Both these effects can be attributed to improved ordering within the crystalline domains.

As shown in Figure 8, the melting endotherms in MDI–BD are much less pronounced than in the 2,6-TDI–BD samples. After 90 min of annealing, the transitions at 94 and 135 °C disappear while the melting endotherm at 202 °C becomes more intense. Longer annealing times resulted in only minor changes in the pos-

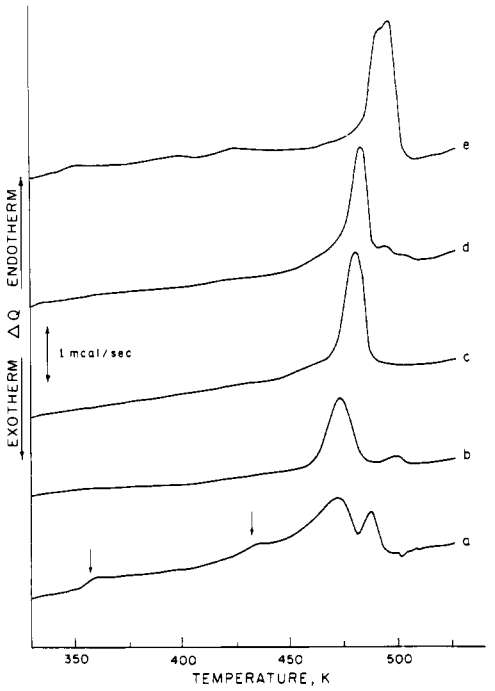

Figure 8. DSC curves for MDI-BD annealed at 150 °C: (a) control; (b) 90 min; (c) 4 h; (d) 8 h; (e) slow solvent evaporation technique.

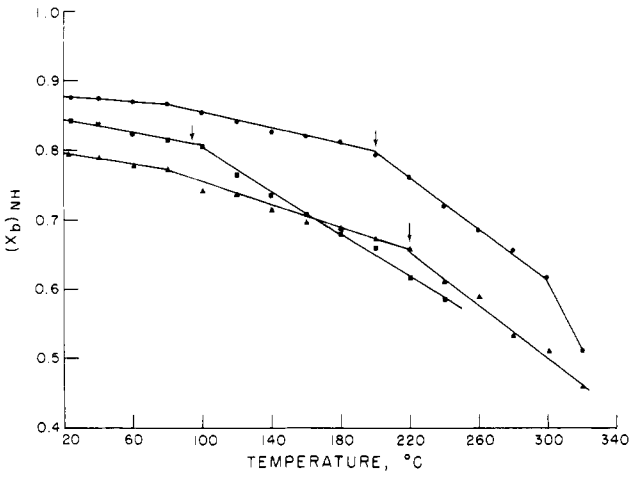

Figure 9. Fraction of hydrogen-bonded N-H (X_b) vs. temperature for model hard-segment compounds: (●) 2,6-TDI-BD; (■) 2,4-TDI-BD; (▲) MDI-BD.

ition and area of this main peak. For the slowly evaporated sample, however, the DSC scan shows two sharp and overlapping peaks at 225 and 231 °C and a corresponding increase in area. No change in the DSC behavior of 2,4-TDI-BD is observed following heat treatment. A summary of these transition temperatures is listed in Table III.

Temperature Dependence of Hydrogen Bonding. To determine whether the dissociation of hydrogen bonding in these treated samples is consistent with the observed spectral changes and DSC behavior, the temperature dependence of the N-H absorption band was investigated. Figure 9 shows a plot of the fraction of hydrogen-bonded N-H (X_b) groups vs. temperature for the fully annealed 2,6- and 2,4-TDI-BD samples and slowly evaporated MDI-BD cast sample. For 2,4-TDI-BD, Figure 6 shows that X_b remains nearly constant below 100 °C (corresponding to T_g) and decreases linearly above this temperature. In 2,6-TDI-BD and MDI-BD, the slope change at T_g is much less pronounced. There is, however, a marked decrease in X_b near the melting temperature

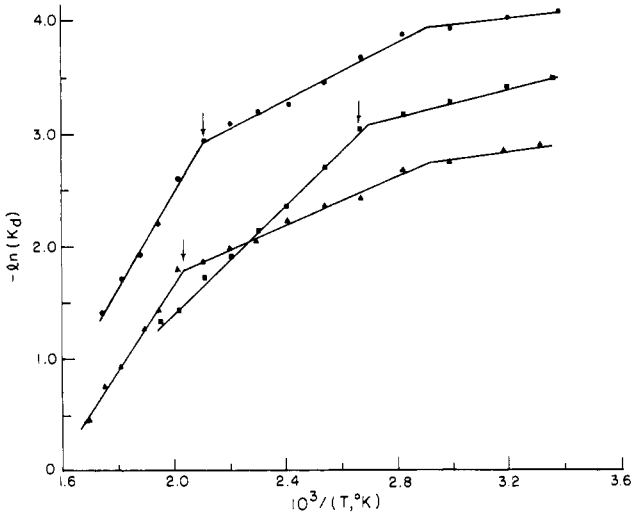

Figure 10. Temperature variation of the hydrogen-bonding equilibrium constant in model hard-segment compounds: (●) 2,6-TDI-BD; (■) 2,4-TDI-BD; (▲) MDI-BD.

Table IV
Enthalpy of Hydrogen Bond Dissociation for Model Hard-Segment Compounds

sample	onset temp, °C	ΔH, kcal/mol of NH
2,4-TDI-BD	100	4.6
2,6-TDI-BD	200	8.4
MDI-BD	220	7.5

which occurs at about 200 °C in 2,6-TDI-BD and 220 °C in MDI-BD. Similar transitions have been reported earlier in nonsegmented polyurethanes based on 2,4-TDI and MDI and α,ω-diols.[16]

From the data shown in Figure 9 the equilibrium constant for the dissociation of hydrogen-bonded N-H groups is determined:

$$K_d = \frac{[\text{N-H}][\text{O=C}]}{[\text{N-H---O=C}]} = \frac{(1 - X_b)^2}{X_b} \quad (1)$$

The change in enthalpy, ΔH, and entropy, ΔS, for hydrogen bond dissociation is then calculated from the temperature dependence of the equilibrium constant:

$$K_d = \exp(-\Delta H/RT + \Delta S/R) \quad (2)$$

Figure 10 is a plot of $-\ln K_d$ vs. $1/T$. It should be noted that these curves exhibit transitions corresponding to those observed on the X_b curves. Values of ΔH were calculated from data above T_g in the 2,4-TDI-BD curve and above T_m in the 2,6-TDI-BD and MDI-BD curves shown in Figure 9. These values are listed in Table IV.

Discussion

A number of studies have reported substantial changes in the N-H stretching vibration in polyurethanes with both temperature[16,21,22] and deformation.[23-25] These spectroscopic changes are undoubtedly correlated to changes in the uniformity and strength of the hydrogen bonds. It has been generally accepted that the shift, $\Delta\nu$, in the stretching frequency of the hydrogen-bonded X-H group (X-H---Y) is a measure of the strength of the hydrogen bond. With increasing hydrogen bond strength, the X-Y distance (R), measured in the solid state by X-ray crystallography, decreases and this decrease is usually accompanied by an increase in the difference between the associated X-H stretching frequency and nonassociated X-H stretching frequency. In fact, a linear relationship between $\Delta\nu$ and

R has been established for a number of hydrogen bonds of different types.[8] For the N–H---O hydrogen bond, bond distances were found to be in the range 2.84–3.10 Å with corresponding $\Delta\nu$ between 170 and 60 cm^{-1}.[9] On the basis of these average values of $\Delta\nu$ and R, Pimentel et al. have derived

$$\Delta\nu = 0.548 \times 10^3(3.21 - R) \quad (3)$$

describing a linear relationship between these two properties. Their data are reasonably consistent with that of Nakamoto, Margoshes, and Rundle[10] and Lord and Merrifield.[8] Changes in the average N–H---O bond distance are also believed to be responsible for intensity variation of the N–H absorption band,[26] while the considerable breadth beyond the inherent width is attributed to the presence of a very large number of differently hydrogen-bonded species with a wide range of N–H---O distances.[27]

The spectral properties $\Delta\nu$, $\Delta\nu_{1/2}$, and B have been examined here for the hydrogen-bonded system N–H---O=C in three hard-segment copolymers. Prior to annealing, these spectral features are nearly indistinguishable. Here the hydrogen bonds assume a wide distribution of lengths and random orientation caused by structural disorder within the system. As shown in the DSC scans, all materials exhibit a well-defined glass transition below 100 °C, a further indication of their highly amorphous nature.

After annealing, the spectral properties of the N–H absorption band as well as DSC behavior vary markedly among the three related polymers. Differences in behavior are attributed to differences in the packing of the structural units. In 2,4-TDI–BD, asymmetric placement of the isocyanate residues with respect to the methyl group can result in head-to-tail isomerization within the repeat units. Variations in the orientation of these units cause immutable chain defects and consequently a noncrystallizable polymer. Thus annealing has no effect on the organization as evidenced by DSC or on the hydrogen-bonding properties as shown by infrared. This behavior is consistent with that observed in the corresponding segmented polyurethane materials.[28]

For 2,6-TDI–BD and to a lesser degree MDI–BD, changes in $\Delta\nu$, $\Delta\nu_{1/2}$, and B values show that hydrogen-bonding properties of the urethane group are markedly affected by annealing. The decrease in the bonded N–H and C=O stretching frequency and the slight increase in amide II and V vibrations indicate that the N–H---O bond is significantly stronger following annealing. This presumably results from reorganization of the chains involving a shortening of the hydrogen bond. This change in bond distance would also be expected to alter the electronic charge distribution of the hydrogen bond and, therefore, the intensity (the intensity being proportional to the square of the change in dipole moment with respect to the vibration). Using eq 1 presented earlier, $\Delta\nu$ in 2,6-TDI–BD and MDI–BD corresponds to an average N–H---O bond distance of 2.90 and 3.02 Å, respectively. These predicted values lie very close to those obtained by X-ray analysis on model hard-segment compounds based on MDI–bis(methylurethane).[29,30] Here it was shown that MDI–urethanes can be formed in various modifications which differ by the type of hydrogen bond present. One modification consisted of strong hydrogen bonds, having a N–H---O bond distance of 2.89 Å, while the other modification consisted of molecules bound by weak hydrogen bonds (2.99 Å). Although no detailed spectroscopic analysis has been carried out for these materials, the frequencies of the bonded components occurred at 3275 and 3325 cm^{-1}, respectively. While these frequencies and bond lengths are in good agreement with those obtained in this present study, additional experimental data using X-ray methods are needed to check the $\Delta\nu$–R correlation further for these materials. It is worth mentioning that the frequency of the bonded N–H component in 2,4-TDI–BD corresponds to a N–H---O bond distance of 2.96 Å. However, it should be recognized that the distribution of bond lengths is far greater in this amorphous system and therefore this value represents only a crude estimate.

An obvious explanation of the narrowness of the N–H band in 2,6-TDI–BD and MDI–BD after annealing is that the degrees of freedom normally responsible for the width have been "frozen out". That these degrees of freedom are not merely low-frequency modes interacting in sum and difference combinations is indicated by the symmetrical narrowing. As in 2,4-TDI–BD, a wide variety of conformations having a range of frequencies (associated with a range of N–H---O distances) are possible in the amorphous 2,6-TDI–BD and MDI–BD solution-cast samples. However, annealing and subsequent crystallization of these latter materials lead to homogenization of the hydrogen bonds. This process, as previously mentioned, is not accompanied by a change in the number of bonded N–H groups. The constancy in the degree of hydrogen bonding suggests that the hydrogen bonds assume a preferred length after annealing and that this is associated with the existence of a single conformation of the chain in the crystalline phase. This line of reasoning may also be applied to the corresponding segmented polyurethanes where hydrogen bonding occurs not only in the amorphous hard-segment regions but also in the soft-segment phase. In this case annealing also results in hard-segment crystallization which in turn leads to improved phase separation with less interphase hydrogen bonding.

These spectral changes outlined above for 2,6-TDI–BD and MDI–BD are consistent with the thermal transition behavior observed by DSC. It will be recalled that the transition at about 90 °C is obvious only in the initial solution-cast samples. Apparently the noncrystalline domain structure converts to the crystalline state during annealing and gives rise to well-defined high-temperature transitions. Furthermore, after annealing, these endotherms increase in magnitude and are shifted to higher temperature. It has been suggested that changes in the shape, size, and position of the melting peak are indicative of changes in the crystallite size and in the perfection of the hard-segment structure.[31,32] Since the packing of molecules is largely influenced by hydrogen bonding,[33] it is not surprising that changes in the hydrogen-bonding properties are also observed. The increase in the melting temperature is consistent with the extra strength contributed by stronger, more uniformly distributed hydrogen bonds and possibly larger crystal size. As previously noted, the melting areas increase in an analogous way to the hydrogen-bonding properties as a function of annealing time. This may also imply a certain contribution of hydrogen bond dissociation to the observed DSC curve. The more pronounced changes observed in 2,6-TDI–BD both by infrared and by DSC are presumably a result of its smaller size and ease with which it crystallizes compared to the MDI–BD polymer.

The temperature dependence of hydrogen bonding in these polymers is also in accord with the above analysis. In 2,4-TDI–BD hydrogen bond dissociation occurs above T_g. It seems reasonable that the onset of segmental motion at T_g will allow a temperature-dependent equilibrium to be established between free and hydrogen-bonded N–H groups in this amorphous polymer. While some dissociation of the bonded N–H groups (<15%) occurs in the

vicinity of T_g for 2,6-TDI–BD and MDI–BD, it is not until the melting point of the polymer is reached that the hydrogen-bonding equilibrium is established. Any dissociation prior to melting may represent the disruption of weaker hydrogen bonds which possibly reside in the less ordered and amorphous regions.

It is also to be noted that ΔH, the enthalpy of hydrogen bond dissociation, is significantly higher in 2,6-TDI–BD and MDI–BD than in 2,4-TDI–BD. The results again suggest that stronger, more uniform hydrogen bonds occur in the ordered crystalline regions.

Conclusions

Changes in the frequency, bandwidth, and intensity of the bonded N–H absorption band following heat treatment have been studied in three model hard-segment polymers and correlated to structural changes as evidenced by DSC. Variations in behavior among the three compounds are attributed to differences in packing and the ability and ease at which crystallization and/or reorganization of the repeat units occur. Annealing of 2,6-TDI–BD and MDI–BD results in a change in distribution toward stronger hydrogen bonds as measured by $\Delta\nu$ and corresponding increase in the melting temperatures. The half-width and intensity of the N–H stretching band also show a strong dependence on annealing time as does the shape and size of the melting endotherms; they narrow and become more intense with longer annealing times. This indicates a uniformity in hydrogen bonds as well as in structure. The insensitivity of the 2,4-TDI–BD copolymer to thermal treatment is the result of poorer hard-segment organization and inability to crystallize. Estimates of N–H---O bond distances obtained from $\Delta\nu$–R correlation are in the range 2.90–3.02 Å, in reasonable agreement with X-ray studies on urethane model compounds. The temperature dependence of hydrogen bonding shows transitions corresponding to T_g in all three polymers and to T_m in 2,6-TDI–BD and MDI–BD. The higher values of ΔH in the latter materials are also consistent with the increased strength of the hydrogen bonds and the higher degree of order present.

The present spectroscopic results on hard-segment copolymers are also significant with work relating to corresponding polyurethane elastomers. It is hoped that in these materials the detailed investigation of the positions and shapes of these bands which are sensitive to the environment of the urethane group, i.e., the N–H stretching frequency near 3300 cm^{-1}, the amide I near 1700 cm^{-1}, the amide II near 1550 cm^{-1}, and the N–H out-of-plane deformation near 700 cm^{-1}, will lead to important structural and chemical information. A subsequent publication will focus on this approach.

Acknowledgment. We are grateful to the Army Materials and Mechanics Research Center, Watertown, MA, for the support of this research under Contract DAAG 46 79C 0004.

References and Notes

(1) Estes, G. M.; Cooper, S. L.; Tobolsky, A. V. *J. Macromol. Sci., Rev. Macromol. Chem.* **1970**, *C4* (1), 167.
(2) Clough, S. B.; Schneider, N. S.; King, A. O. *J. Macromol. Sci., Phys.* **1968**, *2*, 641.
(3) Koutsky, J. A.; Hien, N. V.; Cooper, S. L. *J. Polym. Sci.* **1970**, *8*, 353.
(4) Seymour, R. W.; Estes, G. M.; Cooper, S. L. *Macromolecules* **1970**, *3*, 579.
(5) Bonart, R. *J. Macromol. Sci.* **1968**, *B2* (1), 115.
(6) Bonart, R.; Morbitzer, L.; Hentze, G. *J. Macromol. Sci., Phys.* **1969**, *B3* (2), 337.
(7) Badger, R. M.; Bauer, S. H. *J. Chem. Phys.* **1937**, *5*, 839.
(8) Lord, R. C.; Merrifield, R. E. *J. Chem. Phys.* **1953**, *21*, 166.
(9) Pimentel, G. C.; Sederholm, C. H. *J. Chem. Phys.* **1956**, *24*, 639.
(10) Nakamoto, K.; Margoshes, M.; Rundle, R. E. *J. Am. Chem. Soc.* **1955**, *77*, 6480.
(11) Senich, G. A. Ph.D. Dissertation, University of Massachusetts, 1979.
(12) Huh, D. S.; Cooper, S. L. *Polym. Eng. Sci.* **1971**, *11*, 369.
(13) Lyman, D. *J. Polym. Sci.* **1960**, *45*, 49.
(14) Chang, A. L.; Thomas, E. L. *Adv. Chem. Ser.* **1979**, *No. 176*.
(15) Snyder, R. G.; Schachtschneider, J. H. *Spectrochim. Acta* **1963**, *19*, 85.
(16) MacKnight, W. J.; Yang, M. *J. Polym. Sci., Part C* **1973**, *42*, 817.
(17) Tanaka, T.; Yokoyama, T.; Yamaguchi, Y. *J. Polym. Sci.* **1968**, *6*, 2137.
(18) Paik Sung, C. S.; Schneider, N. S. *Macromolecules* **1977**, *10*, 452.
(19) Senich, G. A.; MacKnight, W. J. *Adv. Chem. Ser.* **1979**, *No. 176*.
(20) Illinger, J. L.; Schneider, N. S.; Karasz, F. E. *Polym. Eng. Sci.* **1972**, *12*, 25.
(21) Srichatrapimuk, V. W.; Cooper, S. L. *J. Macromol. Sci., Phys.* **1978**, *B15* (2), 267.
(22) Senich, G. A.; MacKnight, W. J. *Macromolecules* **1980**, *13*, 106.
(23) Nakayama, K.; Ino, T.; Matsubara, I. *J. Macromol. Sci., Chem.* **1969**, *A3* (5), 1005.
(24) Estes, G. M.; Seymour, R. W.; Cooper, S. L. *Macromolecules* **1971**, *4*, 452.
(25) Ishihara, H.; Kimura, I.; Saito, K.; Ono, H. *J. Macromol. Sci., Phys.* **1974**, *B10* (4), 591.
(26) Finch, J. N.; Lippincott, E. R. *J. Phys. Chem.* **1957**, *61*, 921.
(27) Wall, T. T.; Hornig, D. F. *J. Chem. Phys.* **1965**, *43*, 2079.
(28) Schneider, N. S.; Paik Sung, C. S.; Matton, R. W.; Illinger, J. L. *Macromolecules* **1975**, *8*, 62.
(29) Gardner, K. H.; Blackwell, J. *Polymer* **1979**, *20*, 13.
(30) Hocker, J.; Born, L. *J. Polym. Sci., Polym. Lett. Ed.* **1979**, *17*, 723.
(31) Hesketh, T. R.; van Bogart, J. W. C.; Cooper, S. L. *Polym. Eng. Sci.* **1980**, *20*, 190.
(32) Mandelkern, L. "Crystallization of Polymers"; McGraw-Hill: New York, 1964.
(33) Pimentel, G. C.; McClellan, A. L. "The Hydrogen Bond"; W. H. Freeman: San Francisco, 1960.